Mechanical Anisotropy in Oriented Linear Polyethylene of Various Crystallinities

W. P. LEUNG and C. L. CHOY, *Department of Physics, The Chinese University of Hong Kong, Hong Kong,* and CHANGHUA XU, ZONGNENG QI, and RENJE WU, *Institute of Chemistry, Academia Sinica, Beijing, China*

Synopsis

We have studied the mechanical moduli of oriented linear polyethylene with crystallinities X varying from 0.44 to 0.63 and draw ratios $\lambda = 1$–9 by using a dynamic tensile method at 10 Hz and an ultrasonic technique at 10 MHz. Wide-angle X-ray diffraction and birefringence measurements reveal that the chains in the crystalline regions are fully aligned at $\lambda > 4$, but the degree of amorphous orientation increases steadily up to the highest draw ratio. From -180°C to the β relaxation region (near 0°C at 10 Hz) the mechanical behavior at all crystallinities is controlled by three factors: molecular orientation, weak c-shear deformation and stiffening effect of taut tie molecules. At low temperature the chain alignment in an oriented sample gives rise to an axial Young's modulus E_o which is much larger than the transverse Young's modulus E_{90}, with the modulus for the undrawn material lying in-between. However, the results that $E_{45} < E_{90}$ and C_{44} (axial shear modulus) $< C_{66}$ (transverse shear modulus) imply that a weak c-shear process occurs even at low temperature. At the β relaxation where the amorphous regions are rubbery, the stiffening effect of taut tie molecules becomes prominent and leads to increases in all moduli upon drawing. For the polyethylene with the lowest cyrstallinity a strong c-shear process is activated at the α relaxation (about 50°C at 10 Hz), which gives rise to very low values of C_{44} and E_{45}. This effect becomes weaker with increasing crystallinity and is hardly observable at $X > 0.6$.

INTRODUCTION

In recent years, commercial processes have been developed to produce linear polyethylene of density varying from 0.915 to 0.96 g/cm^3 (crystallinity $\simeq$ 0.4–0.7) by the compolymerization of ethylene with a small amount of α-olefin such as 1-butene.[1] The materials in the lower density range (0.915–0.935 g/cm^3) are known as linear low-density polyethylene (LLDPE). Compared to branched low-density polyethylene, LLDPE has higher stiffness and tensile strength at a given density and improved heat and stress crack resistance. Moreover, because of its linear chain structure LLDPE is more readily stretched to high draw ratios, giving materials of high mechanical modulus and strength.

In a recent study[2] of oriented LLDPE we have identified three major factors which control the mechanical properties, namely, chain orientation, stiffening effect of taut tie molecules, and shear deformation along the chain direction in planes containing the chain axis (c-shear mechanism). When linear polyethylene is drawn the molecular chains in both the crystalline and amorphous regions rotate progressively toward the draw direction. Simultaneously, the crystalline lamellae are broken into smaller blocks which are connected by axially aligned tie molecules originating from the partial unfold-

Journal of Applied Polymer Science, Vol. 36, 1305–1324 (1988)
 CCC 0021-8995/88/061305-20$04.00

ing of chains. This material with highly oriented chains exhibits anisotropic mechanical behavior, notably that its axial Young's modulus E_o is much higher than the transverse modulus E_{90}. Moreover, the presence of taut tie molecules gives rise to a considerable constraint on the other chain segments in the amorphous regions. Though hardly noticeable at low temperature the constraining effect becomes increasingly important as temperature rises, and is very prominent at room temperature where the amorphous phase is in a rubbery state. As a result, even the transverse Young's (E_{90}) and shear (C_{66}) modulus increase significantly upon drawing. At yet higher temperatures (near the α relaxation) a strong c-shear process is activated, leading to very small values for the axial shear modulus C_{44} and the Young's modulus at 45° to the draw direction E_{45}.

It is expected that the relative importance of these three factors may change with increasing crystallinity, but there has been very little work in this area. In an attempt to reveal the interplay of the effects of orientation and crystallinity we have studied the mechanical properties of uniaxially oriented linear polyethylene samples prepared from isotropic materials having three different crystallinities: $X = 0.44$, 0.52 and 0.59. The Young's moduli E_o, E_{45}, and E_{90} were determined from $-180°$ to 100°C using a dynamic tensile apparatus at 10 Hz and the five independent elastic moduli were measured from $-60°$ to 60°C by an ultrasonic method at 10 MHz. Wide-angle X-ray diffraction and birefringence measurements were also carried out so as to provide an estimate of the degree of chain orientation in the crystalline and amorphous regions.

EXPERIMENTAL

Sample Preparation

The starting material is a series of ethylene/1-butene copolymers (Sclair 91A, 94D, and 96A) produced commercially by DuPont Canada Inc. using a low pressure solution process. The number and weight-average molecular weights and the approximate number of side groups per 1000 carbon atoms are given in Table I.[3]

Pellets of these linear polyethylene samples were compression molded at 160°C into 3-mm thick sheets and then quenched in water at room temperature. Oriented samples were prepared by drawing the isotropic sheets at 65°C on a Instron tensile machine at a rate of 1 cm/min. The polymer with the lowest crystallinity, Sclair 91A, deforms almost homogeneously below a draw ratio of $\lambda = 3.6$, at which point necking occurs. It was thus possible to prepare

TABLE I
Characteristics of the Polyethylenes Studied

Trade name	$M_n \times 10^{-3}$	$M_w \times 10^{-3}$	Approximate number of side groups per 1000 C atoms
Sclair 91A	23.7	123	20
Sclair 94D	26.8	110	6
Sclair 96A	17.8	193	2.5

samples in the full range of $1 < \lambda < 6.1$. For samples of higher crystallinity the necking was very sharp, and so only samples above the "natural" draw ratio of about 4.4 (Sclair 94D) and 5.6 (Sclair 96A) could be prepared. Moreover, the strain-hardening effect at high draw ratios increases rapidly with the decrease of crystallinity.[4] Consequently, in the drawing of Sclair 91A and 94D to high strains, there was a serious problem of slippage at the grips. Therefore we had not been able to prepare highly drawn samples of sufficient width (~ 4 cm) for low-frequency dynamic mechanical measurements along the transverse direction.

Sample Characterization

The samples were examined under a Leitz optical microscope with crossed polarizers. The density ρ of the samples was determined by the flotation method and the volume fraction crystallinity X_ρ was calculated from:

$$X_\rho = \frac{\rho - \rho_a}{\rho_c - \rho_a} \tag{1}$$

where $\rho_c = 1.000$ and $\rho_a = 0.855$ g/cm^3 are the densities of the crystalline and amorphous phases.[5] Following a common practice[6] we had assumed that ρ_a remains unchanged upon drawing.

The melting endotherms were recorded at a heating rate of 10°C/min using a Perkin-Elmer DSC-2 differential calorimeter. The enthalpy of fusion H was measured and the volume fraction crystallinity X_H was calculated from the expression:

$$X_H = \frac{\rho H}{\rho_c H_c} \tag{2}$$

where the enthalpy of fusion of polyethylene crystals H_c is taken to be 69 cal/g.[7]

Wide-Angle X-Ray Diffraction and Birefringence

The azimuthal intensity distribution of the x-ray reflection from the (002) planes was recorded with a Syntex R3 diffractometer and the crystalline orientation function f_c was obtained by integrating the intensity over all angles.[8] Birefringence measurements were carried out at room temperature with a Leitz polarizing microscope equipped with a tilting compensator.

Mechanical Measurements

Dynamic tensile measurements at 0°, 45°, and 90° to the draw axis were made at 10 Hz on a viscoelastic spectrometer (Iwamoto Seisakusho) from −180 to 100°C. For the 45° and 90° measurements, the samples exhibited serious creep at high temperatures and so the upper temperature limits for these measurements were lower (60–80°C). The typical size of the samples was $40 \times 2 \times 0.8$ mm^3, with the largest dimension lying along the direction of the applied stress.

The five independent elastic moduli C_{11}, C_{13}, C_{33}, C_{44}, and C_{66} were determined at 10 MHz from -60 to 60°C using an ultrasonic technique described previously.[9] Typical size of the samples was $14 \times 10 \times 0.8$ mm^3, with the largest dimension lying along the draw direction. To avoid structural changes during measurement the samples had been annealed previously for 2 h at 60°C, the upper temperature limit of our measurements. From these elastic moduli other mechanical parameters such as the Young's modulus and Poisson's ratios could be calculated.

RESULTS AND DISCUSSION

Crystallinity and Orientation

Under a polarizing microscope, the undrawn samples of Sclair 91A, 94D, and 96A exhibited a spherulitic morphology, with the diameter of the spherulites varying from 3 to 20 μm. As the sample was drawn, the spherulites were deformed and then broken up. For Sclair 91A the spherulites disappeared completely at a draw ratio $\lambda \geq 2.6$, indicating the formation of a microfibrillar structure. Sclair 94D and 96A showed very sharp necking behavior and the "natural" draw ratios in the neck were 4.4 and 5.6, respectively. At or above these draw ratios the samples have a fibrillar morphology.

As shown in Table II there is an increase in the crystallinity X_ρ accompanying the transformation from spherulitic to fibrillar morphology. Further drawing leads to shear deformation of the microfibrils and an accompanying increase in the crystallinity. As expected, the strain-induced crystallization effect is more significant for polymers of lower crystallinity, as is evident by comparing the crystallinity data for the three polymers (Table II). It should be noted, however, that the calculation of X_ρ is based on the assumption of constant density for the amorphous phase, which may not be valid at high draw ratio. Nevertheless, the heat of fusion measurement also gives a crystallinity X_H which shows the same trend as X_ρ.

TABLE II
Characteristics of Oriented Polyethylene Samples

Trade name	λ	ρ (g/cm^3)	X_ρ	X_H	$\Delta \times 10^4$
Sclair 91A	1	.919	.441	.381	0
	2.6	.920	.448	.390	283
	3.6	.921	.455	.400	336
	4.9	.923	.469	.426	374
	6.1	.925	.483	.430	411
Sclair 94D	1	.930	.517	.435	0
	4.4	.933	.538	.457	383
	5.8	.935	.552	.479	421
	8	.941	.593	.513	445
	9	.943	.607	.524	461
Sclair 96A	1	.940	.586	.540	0
	5.6	.941	.593	.549	427
	7	.943	.607	.558	448
	9	.946	.628	.586	466

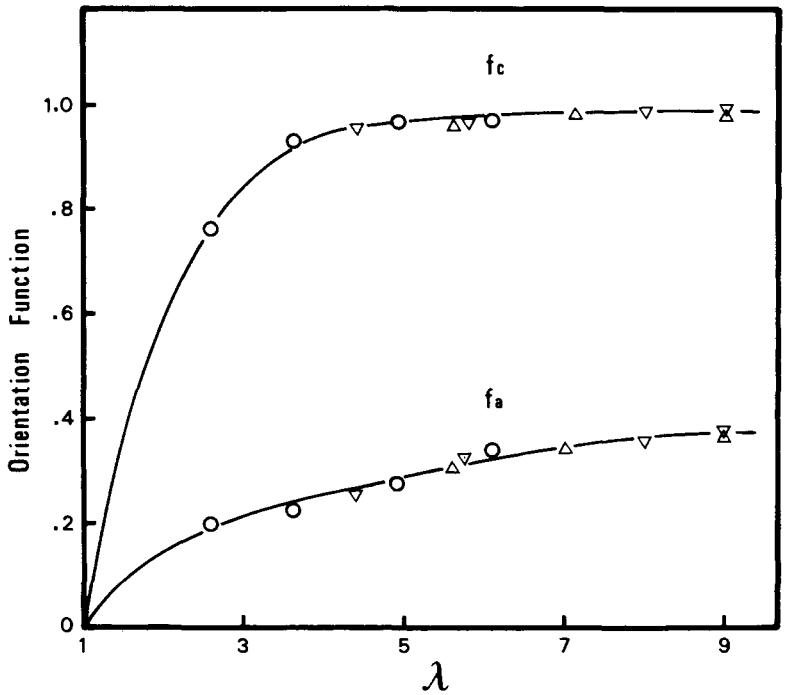

Fig. 1. Draw ratio dependence of the crystalline (f_c) and amorphous (f_a) orientation functions for oriented polyethylene. Sclair 91A (○), Sclair 94D (▽), Sclair 96A (△).

Figure 1 shows that the crystalline orientation function f_c increases sharply in the range $\lambda = 1$–3 and approaches saturation at higher λ. Thus the chains in the crystalline regions are essentially aligned at $\lambda > 4$. However, as reflected by the steady increase in the birefringence given in Table II, the degree of orientation in the amorphous phase keeps on rising as λ increases from 4 to 9. Neglecting form birefringence, the amorphous orientation function f_a can be calculated from the observed birefringence using the equation:[10]

$$\Delta = Xf_c\Delta_c^\circ + (1 - X)f_a\Delta_a^\circ \tag{3}$$

where Δ_c° and Δ_a° are the intrinsic birefringences of the crystalline and amorphous phases, and X is the crystallinity deduced from the density. The generally accepted value of Δ_c° is 0.0585,[11] but several values[12–14] have been suggested for Δ_a°. We have previously discussed[2] in detail the relative merits of these values and have concluded that the Δ_a° value of 0.074 calculated theoretically by Pietralla et al.[14] seems to be the most reasonable. Using these intrinsic birefringences f_a has been calculated and found to increase steadily over the entire draw ratio range, reaching a value of 0.4 at $\lambda = 9$ (see Fig. 1). It should be noted that f_a is contributed by all the chain segments in the amorphous phase, which include tie molecules, loops, cilia, and floating chains.

Low-Frequency Mechanical Measurements

Figure 2 shows the loss tangent $\tan\delta$ and loss modulus E'' for the three polymers, Sclair 91A, 94D, and 96A, as functions of temperature. For Sclair

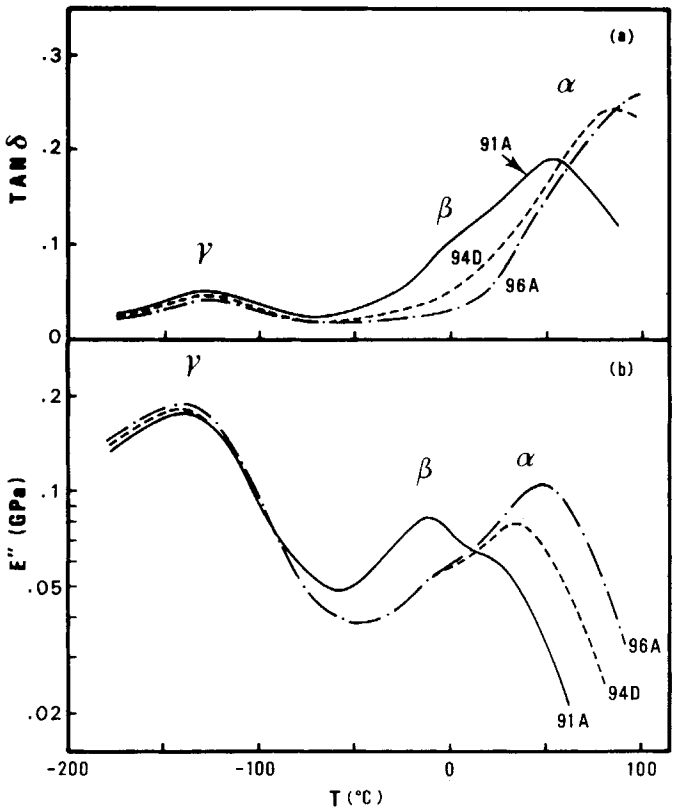

Fig. 2. Temperature dependence of the (a) loss tangent and (b) loss modulus for isotropic polyethylene.

91A, three relaxations are observed in both the tan δ and E'' plots. However, the β process appears only as a shoulder in the tan δ plot whereas the same is true for the α process in the E'' plot. For the polymers with higher crystallinity, Sclair 94D and 96A, the β relaxation is so weak that it is barely noticeable in the E'' plot and is completely absent from the tan δ plot. We also note that the α peak shifts to high temperature as the crystallinity increases.

It is generally agreed that the γ relaxation is related to localized chain motions in the amorphous phase,[15,16] and there are evidences that the β process may involve the motion of chain segments in the amorphous[16] and interfacial[17] regions. In ethylene/1-butene copolymers, the crystal growth is limited by the exclusion of the ethyl branches of the comonomer from the crystal. Therefore, the interfacial regions will contain a high fraction of such branches which will affect its local glass transition temperature (T_g) and the consequent β relaxation. It is also well known that the α process observed by nuclear magnetic resonance (NMR) and dielectric techniques occurs within the crystallites.[15,16] However, the motions in the crystallites can be transmitted to the amorphous regions since the ends of amorphous chain segments, including tie molecules, loops, and cilia, are anchored at the crystallites. Therefore, the mechanical α process is a concerted process involving both the

crystalline and amorphous regions and the rate-determining process occurs within the crystal or at its defects and grain boundaries.

In this section we will discuss mainly the behavior of the Young's modulus at various directions to the draw axis. The loss tangent, associated with the energy loss in the sample, has been included for completeness. The Young moduli E_o, E_{45}, and E_{90} for an oriented Sclair 91A sample ($X_\rho = 0.47$, $\lambda = 4.9$) are shown as functions of temperature in Figure 3. Below the γ relaxation the axial Young's modulus E_o is much higher than the transverse modulus E_{90}, with the modulus for the undrawn sample ($\lambda = 1$) lying in between, implying that the mechanical behavior is determined largely by the overall molecular orientation. However, the result that E_{45} is slightly smaller than E_{90} indicates that a weak c-shear process may contribute even at low

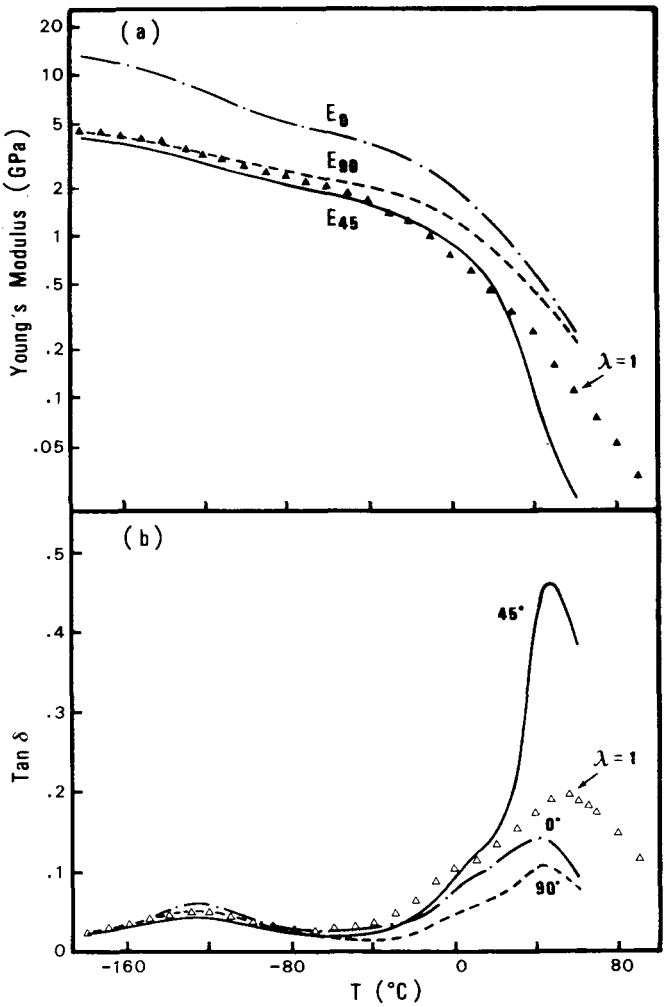

Fig. 3. Temperature dependence of the (a) Young's modulus and (b) loss tangent for oriented Sclair 91A ($\lambda = 4.9$) at 0°, 45°, and 90° to the draw axis measured at 10 Hz. Data points for isotropic Sclair 91A are included for comparison.

temperatures. In the β transition region (-20 to 20°C) both E_{45} and E_{90} are higher than the modulus of the isotropic sample, indicating that the amorphous phase is reinforced by the taut tie molecules produced in the drawing process.

At yet higher temperatures (near the α relaxation), a strong c-shear process comes into play. This process, which involves the shear deformation in planes containing the chain axis, leads to a drastic decrease in E_{45} and an accompanying rise in the loss tangent. A sharp drop in the axial shear modulus was also observed in our previous work,[2] which is consistent with the assignment of c-shear mechanism. These features were first observed in branched low-density polyethylene by Raumann and Saunders[18,19] and were subsequently studied in detail by Ward and co-workers.[20-22] The factor affecting the c-shear process is the ability of chains to rotate about and translate along their c-axis. This is related to the crystal perfection and thickness which are influenced by branching.

As the crystallinity increases the mechanical behavior below 20°C remains essentially unchanged but the c-shear process becomes much weaker (see Figs. 3–5). If we use E_{90}/E_{45} as a rough measure of the strength of this mechanism, then the values of this ratio at 60°C are, respectively, 10, 3 and 1.5, for Sclair 91A, 94D and 96A in the draw ratio range of 4.4–5.6. The relaxation strength is further reduced if the draw ratio is increased. For a Sclair 96A sample at $\lambda = 9$, E_{45} is only 30% lower than E_{90} even at a high temperature of 80°C (see Fig. 6). This result is consistent with the work of Ward and co-workers[21,22] which shows that the c-shear process is not important in high-density polyethylene. In fact, the α relaxation in high-density polyethylene is related to an interlamellar shear process.[22]

In conclusion, although the c-shear mechanism is certainly related to the crystalline orientation, the strength of this process is affected strongly by the crystalline content and tie molecule fraction in the sample. The reduction in relaxation strength with increasing crystallinity or tie molecule fraction probably reflects the lowering of molecular mobility in the amorphous and interfacial regions as a result of the constraining effects of crystallites and taut tie molecules.

The draw ratio dependence of the Young's modulus at three selected temperatures, -140°C (just below the γ relaxation), 20°C (between the α and β relaxations), and 60°C (near the α relaxation) is shown for Sclair 91A, 94D, and 96A in Figures 7 to 9, respectively. The features at -140° and 20°C are essentially the same for all three polymers. At -140°C there is a steep rise in E_o and a slight drop in both E_{45} and E_{90} with increasing λ. The behavior of E_o and E_{90} reflects the increase in the degree of orientation in the crystalline (f_c) and amorphous (f_a) regions. As the temperature increases to 20°C the stiffness of the amorphous phase drops substantially, and so the reinforcing effect of taut tie molecules becomes prominent, giving rise to the increase in E_{45} and E_{90}.

The most remarkable feature at 60°C is the very low E_{45} value for Sclair 91A and 94D at $\lambda \simeq 5$, which we have already attributed to a c-shear mechanism. Figure 7 reveals that there is a decrease in E_{45} as λ increases from 3.6 to 4.9, which relates to the further increase in crystalline orientation. For Sclair 94D (Fig. 8), a minimum is observed near $\lambda = 4.4$. At this draw ratio the crystalline chains are already aligned. With further increase in draw

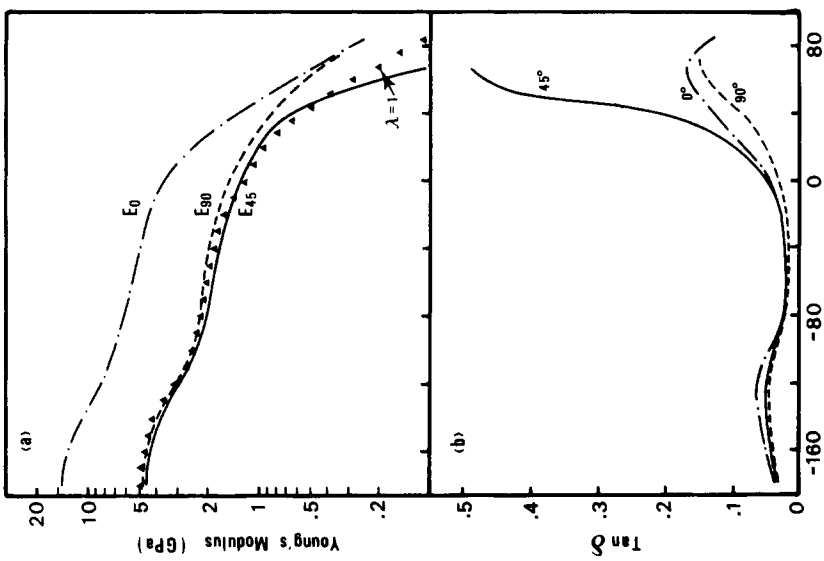

Fig. 4. Temperature dependence of the (a) Young's modulus and (b) loss tangent for oriented Sclair 94D ($\lambda = 4.4$) at 0°, 45°, and 90° to the draw axis measured at 10 Hz. Data points for isotropic Sclair 94D are included for comparison.

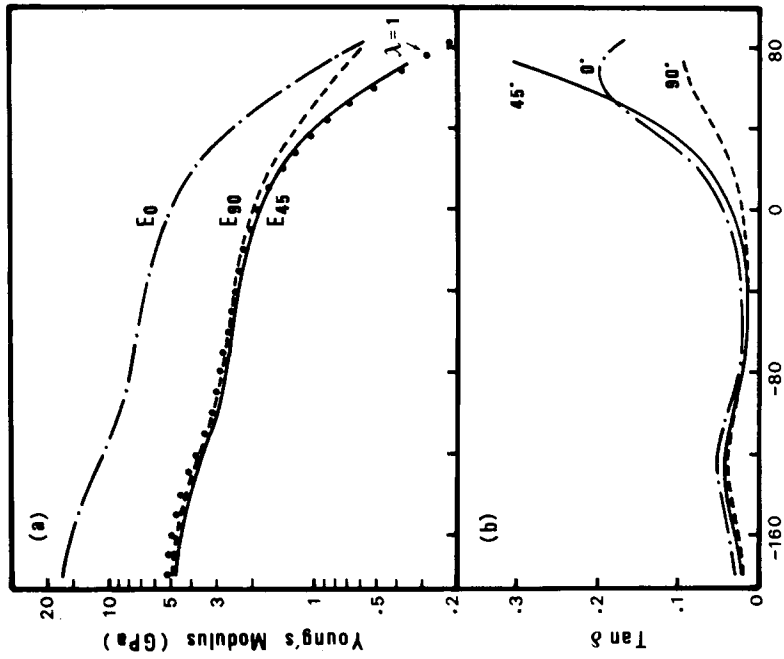

Fig. 5. Temperature dependence of the (a) Young's modulus and (b) loss tangent for oriented Sclair 96A ($\lambda = 5.6$) at 0°, 45°, and 90° to the draw axis measured at 10 Hz. Data points for isotropic Sclair 96A are included for comparison.

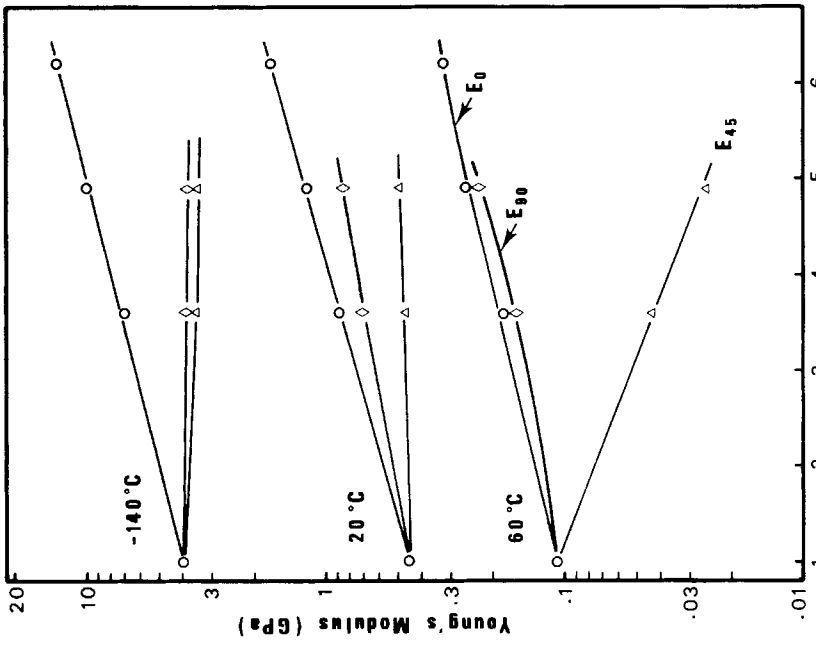

Fig. 7. Draw ratio dependence of the Young's modulus at 10 Hz for oriented Sclair 91D at −140, 20, and 60°C. E_o (○), E_{45} (△), E_{90} (◇).

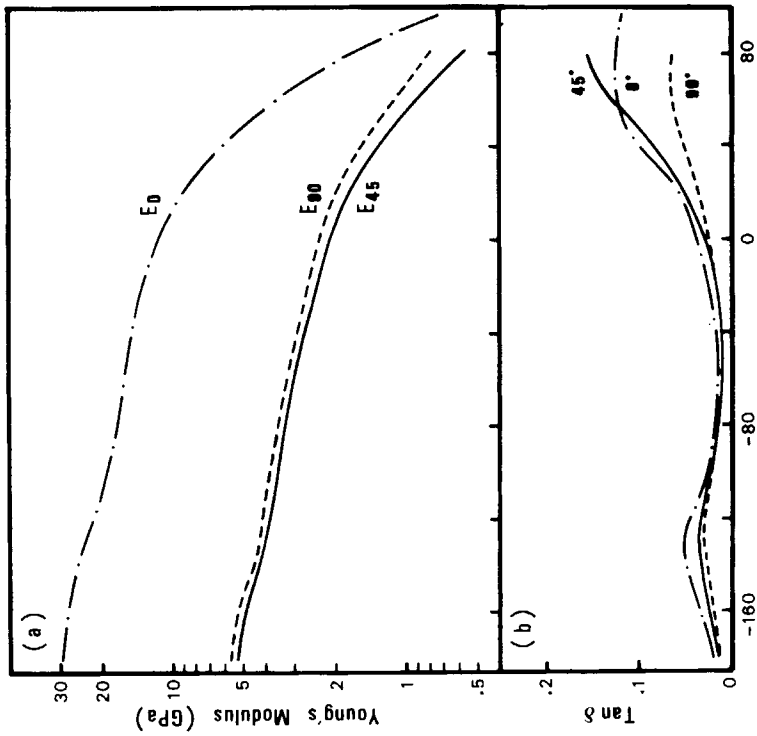

Fig. 6. Temperature dependence of the (a) Young's modulus and (b) loss tangent for oriented Sclair 96A (λ = 9) at 0°, 45°, and 90° to the draw axis measured at 10 Hz.

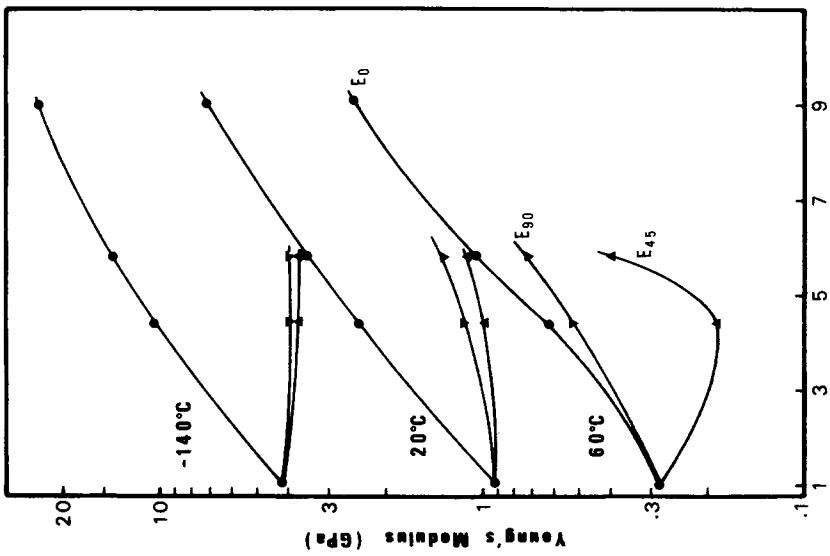

Fig. 8. Draw ratio dependence of the Young's modulus at 10 Hz for oriented Sclair 94D at −140, 20, and 60°C. E_o (●), E_{45} (▲), E_{90} (▼).

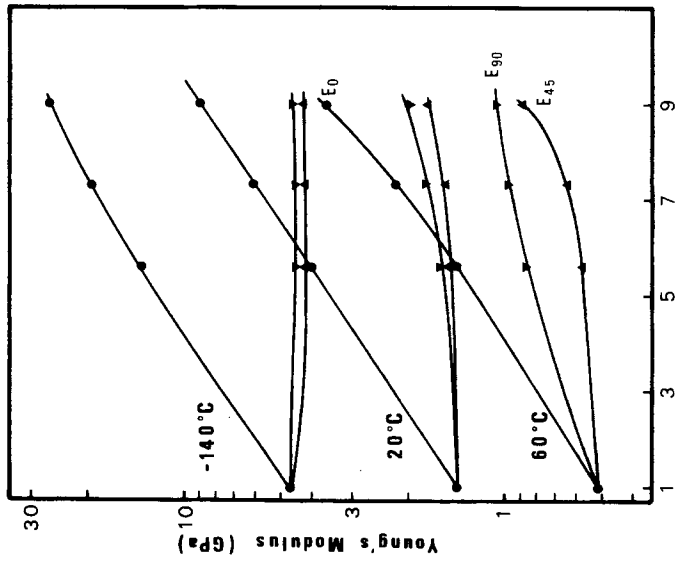

Fig. 9. Draw ratio dependence of the Young's modulus at 10 Hz for oriented Sclair 96A at −140, 20, and 60°C. E_o (●), E_{45} (▲), E_{90} (▼).

ratio both the crystalline content and taut tie molecule fraction increase, thereby leading to a more severe restriction on the segmental motion in the amorphous phase and a consequent increase in E_{45}. The c-shear contribution is not important for highly crystalline Sclair 96A (Fig. 9) and so E_{45} for all oriented samples is larger than the modulus for the undrawn material.

Ultrasonic Moduli

The advantage of the ultrasonic method is that all five independent elastic moduli can be determined by using a small sample which can be readily prepared even at very high draw ratios. A major disadvantage is the strong attenuation of shear waves at such high frequencies, thereby setting a high temperature limit for successful measurements. The upper limit is 60°C for Sclair 91A but is 30–50°C higher for the samples of higher crystallinity (Sclair 94D and 96A). We have carried out measurements only up to 60°C since data for all three polymers are required for the purpose of comparison.

As an illustration, Figure 10 shows the temperature dependence of the five independent elastic moduli C_{11}, C_{13}, C_{33}, C_{44}, and C_{66}, and a related modulus C_{12} ($= C_{11} - 2C_{66}$) for a Sclair 94D sample at $\lambda = 9$. The fact that the axial extensional modulus C_{33} is much larger than the transverse modulus C_{11} and that the cross-plane modulus C_{13} is slightly higher than C_{12} is again a reflection of the chain orientation. However, a purely molecular alignment

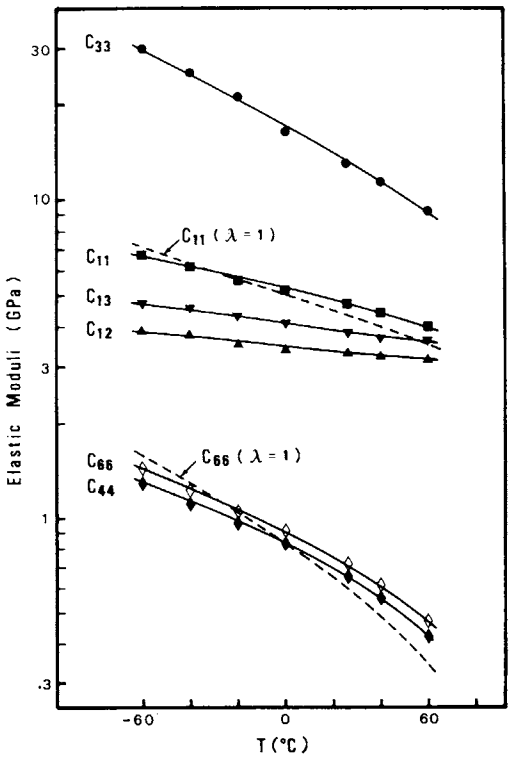

Fig. 10. Temperature dependence of the ultrasonic elastic moduli for oriented Sclair 94D ($\lambda = 9$). The elastic moduli of isotropic Sclair 94D are shown as dashed lines.

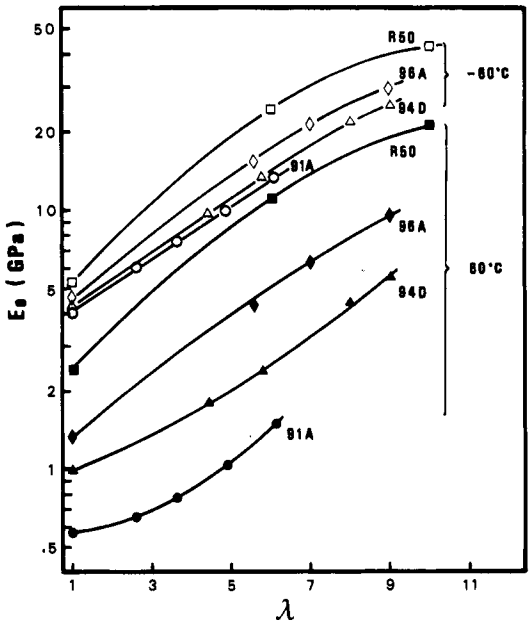

Fig. 11. Comparison of the draw ratio dependence of the ultrasonic axial Young's modulus E_o for four polyethylenes (Sclair 91A, 94D, and 96A, and Rigidex 50).

effect would lead to an axial shear modulus which is higher than the transverse shear modulus,[9,23] and thus is inconsistent with the observed feature: $C_{44} < C_{66}$. To account for this result and our previous observation that $E_{45} < E_{90}$ we suggest that a weak c-shear process is operating even at temperatures much below the α relaxation.

It is not strictly legitimate to compare the low (10 Hz) and high-frequency (10 MHz) moduli by shifting one set of data along the temperature axis according to the time-temperature equivalence principle. This is because polyethylene exhibits three relaxations, each of which has a different activation energy. However, at temperatures near the relaxation peaks, we can use the observed relaxation peak positions at these two frequencies to establish a rough equivalence. According to this criterion, the ultrasonic Young's moduli at -60°C and 60°C should be comparable to the low-frequency moduli at -140°C and 20°C, respectively. A comparison of the ultrasonic (Figs. 11–13) and low-frequency (Figs. 7–9) data shows that the Young's moduli at two vastly different frequencies not only follow the same draw ratio dependence but also have values differing by less than 15% on the average, if a temperature shift is applied in accordance with the time-temperature equivalence rule.

For comparison, our previous data[24] for highly crystalline polyethylene (Rigidex 50, $X \simeq 0.8$) have been included in Figures 11 to 13. It is seen from Figure 11 that the slope of the curves increases with increasing crystallinity, that is, a sample of higher crystallinity has a larger E_o when it is drawn to the same draw ratio. For example, as λ increases from 1 to 9, E_o at 60°C increases by a factor of 8 for the case of Rigidex 50 ($X \simeq 0.8$), as compared to a factor of 5.5 for Sclair 94D ($X \simeq 0.6$). Therefore, if stiffness enhancement is the

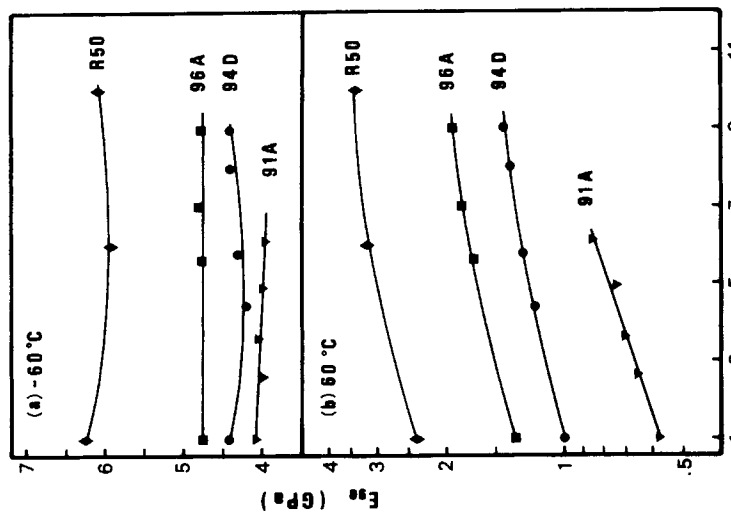

Fig. 13. Comparison of the draw ratio dependence of the ultrasonic Young's modulus E_{90} for four polyethylenes (Sclair 91A, 94D, and 96A, and Rigidex 50). (a) −60 and (b) 60°C.

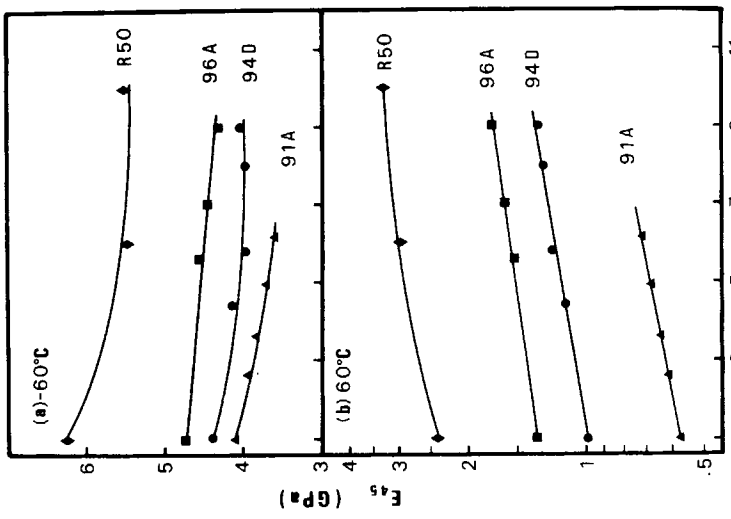

Fig. 12. Comparison of the draw ratio dependence of the ultrasonic Young's modulus E_{45} for four polyethylenes (Sclair 91A, 94D, and 96A and Rigidex 50). (a) −60 and (b) 60°C.

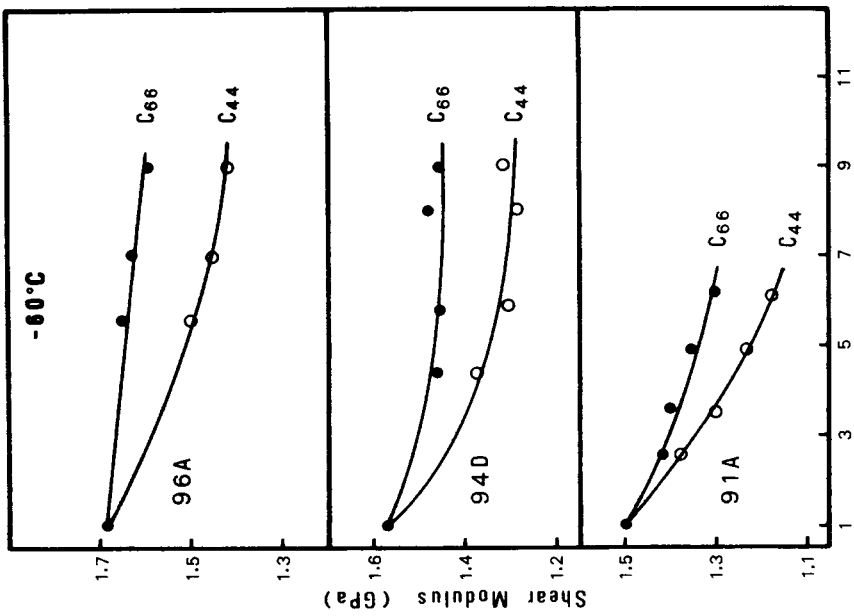

Fig. 15. Draw ratio dependence of the ultrasonic axial shear modulus C_{44} and transverse shear modulus C_{66} for Sclair 91A, 94D, and 96A at −60°C.

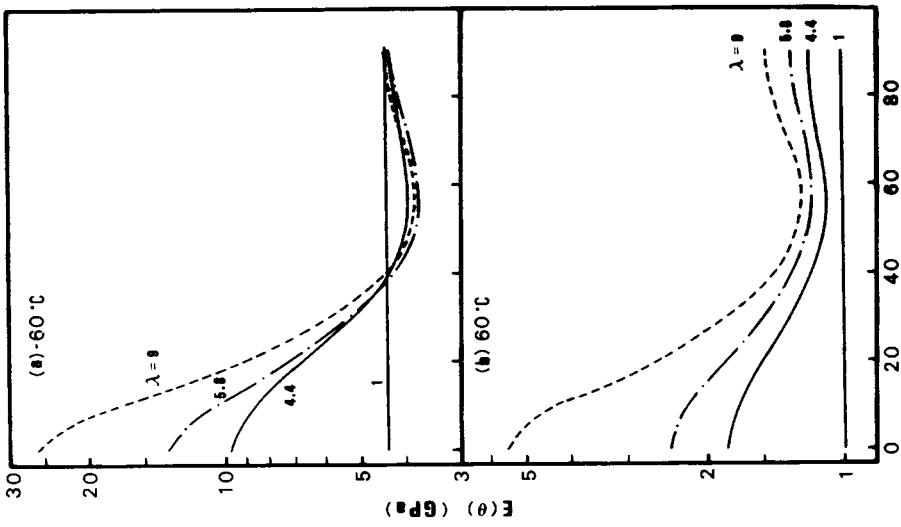

Fig. 14. Variation of the ultrasonic Young's modulus of oriented Sclair 94D as a function of angle relative to the draw direction. (a) −60 and (b) 60°C.

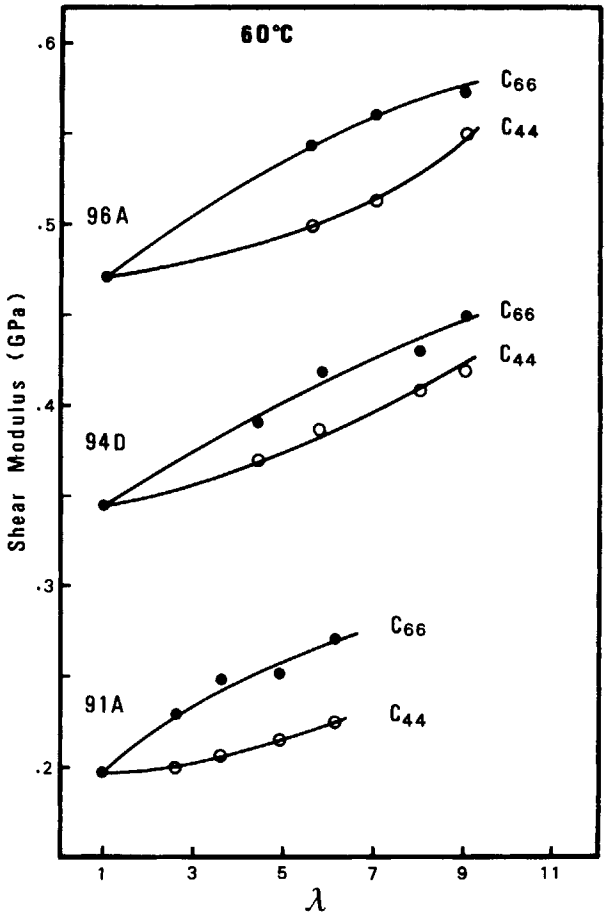

Fig. 16. Draw ratio dependence of the ultrasonic axial shear modulus C_{44} and transverse shear modulus C_{66} for Sclair 91A, 94D, and 96A at 60°C.

major consideration, one should use a material of the highest possible crystallinity.

With the knowledge of the five independent elastic moduli, the Young's modulus at any angle θ relative to the draw direction, E_θ, can be calculated. As an example, Figure 14 shows E_θ as a function of θ for Sclair 94D. At all temperatures a minimum is observed at an angle of about 55°. At 60°C (just above the β relaxation), the Young's modulus of oriented polyethylene at all angles is higher than that for the undrawn material, indicating the importance of the stiffening effect of the tie molecules. Similar features are also observed for Sclair 91A and 96D.

The anisotropy in the shear modulus is shown in Figures 15 and 16. The axial shear modulus C_{44} is lower than the transverse shear modulus C_{66} at all draw ratios and over the entire temperature range, which reflects the contribution of a c-shear process. The decrease of C_{66} with increasing draw ratio at low temperature is related to the progressive alignment of molecular chains.

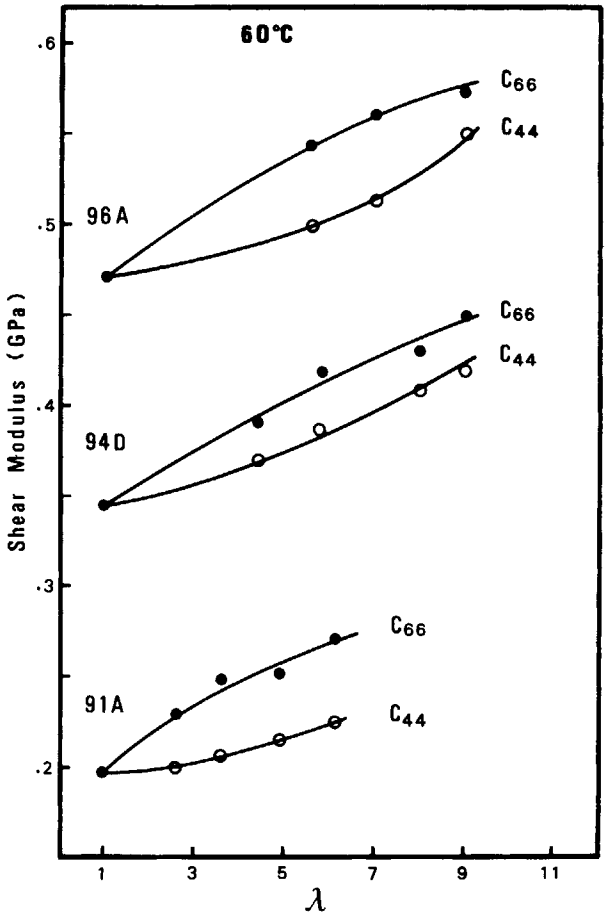

Fig. 16. Draw ratio dependence of the ultrasonic axial shear modulus C_{44} and transverse shear modulus C_{66} for Sclair 91A, 94D, and 96A at 60°C.

major consideration, one should use a material of the highest possible crystallinity.

With the knowledge of the five independent elastic moduli, the Young's modulus at any angle θ relative to the draw direction, E_θ, can be calculated. As an example, Figure 14 shows E_θ as a function of θ for Sclair 94D. At all temperatures a minimum is observed at an angle of about 55°. At 60°C (just above the β relaxation), the Young's modulus of oriented polyethylene at all angles is higher than that for the undrawn material, indicating the importance of the stiffening effect of the tie molecules. Similar features are also observed for Sclair 91A and 96D.

The anisotropy in the shear modulus is shown in Figures 15 and 16. The axial shear modulus C_{44} is lower than the transverse shear modulus C_{66} at all draw ratios and over the entire temperature range, which reflects the contribution of a c-shear process. The decrease of C_{66} with increasing draw ratio at low temperature is related to the progressive alignment of molecular chains.

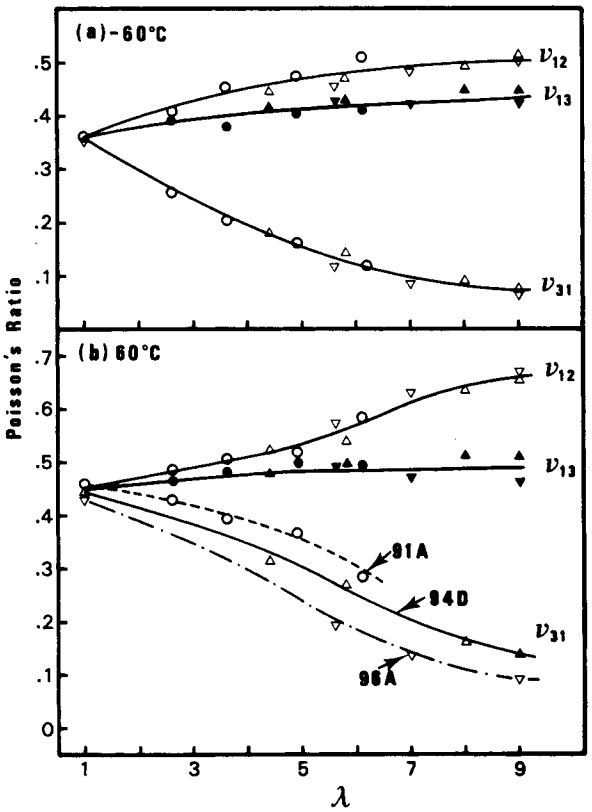

Fig. 17. Draw ratio dependence of the Poisson's ratios for three polyethylenes at (a) −60 and (b) 60°C. Sclair 91A (○, ●), Sclair 94D (△, ▲), Sclair 96A (▽, ▼).

At 60°C, however, the stiffening effect of tie molecules becomes dominant, thereby leading to an increase in both C_{66} and C_{44} upon drawing.

Figure 17 shows the Poisson's ratios of Sclair 91A, 94D, and 96A as functions of draw ratio. Within experimental accuracy, ν_{12} and ν_{13} at all temperatures, and ν_{31} at −60°C fall on the same curves irrespective of crystallinity. However, ν_{31} at 60°C splits into three curves, with the samples of higher crystallity having lower values. This result implies that the stiffening effect is stronger for polymers of higher crystallinity so that, under transverse stretching, the more crystalline sample will deform less along the draw direction. Although ν_{12} is larger than ν_{13} at all draw ratios and temperatures, both of these quantities have values close to 0.5 at 60°C for draw ratios between 3 and 5. This is consistent with the data for a branched low-density polyethylene sample ($\lambda = 3.8$) obtained by quasistatic measurements at room temperature.[25]

Comparison with Composite Model

The mechanical behavior of isotropic and oriented crystalline polymers is commonly analyzed in terms of composite models[26-30] which are based on

similar ideas. For application to oriented polymers the model of McCullough et al.[29] is most appropriate. We will only briefly describe this model since a detailed discussion has been given in our previous work on LLDPE.[2] In this model, a crystalline polymer is regarded as consisting of crystalline and amorphous aggregates of anisotropic units. These units have constant mechanical properties but are gradually aligned as the polymer is drawn. The elastic constants of each aggregate (crystalline or amorphous) can be calculated through an averaging procedure which takes into account the orientation of the units and the internal stress–strain distribution. Finally, the elastic tensor of the polymer can be obtained by the volume-averaging of the properties of the crystalline and amorphous aggregates consistent with the stress-strain field between the aggregates.

A serious drawback of this model is that there is no theoretical framework or experimental technique which can give the internal stress-strain distribution in semicrystalline polymers. Therefore, McCullough et al. were forced to use either the Reuss averaging (assuming uniform stress), which gives the lower bound or the Voigt averaging (assuming uniform strain), which gives the upper bound. However, the upper and lower bounds are too far apart to serve as practical brackets for the moduli. To remedy this situation they followed the approach of Halpin and Tsai[31] by introducing a contiguity factor ξ associated with the internal stress (or strain) distribution. A value of $\xi = 0$ yields the Reuss average whereas a value of $\xi = \infty$ yields the Voigt average. For any specific mechanical model based on the morphology of the polymer such as the Takayanagi model,[32] the value of ξ can be estimated.[29]

For oriented polymers with a fibrillar morphology, as in the present work, it is generally recognized[33] that the Takayanagi model (Fig. 18) is a good starting point for explaining the mechanical properties. In this model the fully oriented crystalline block is coupled in series to the amorphous region and this combination is then coupled in parallel to the aligned tie molecules. Since there is no evidence for the existence of crystalline bridges in oriented

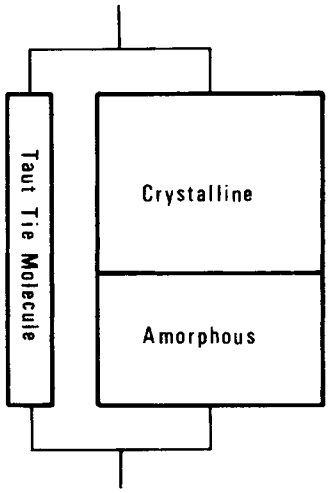

Fig. 18. Schematic diagram of the Takayanagi model for highly oriented crystalline polymers.

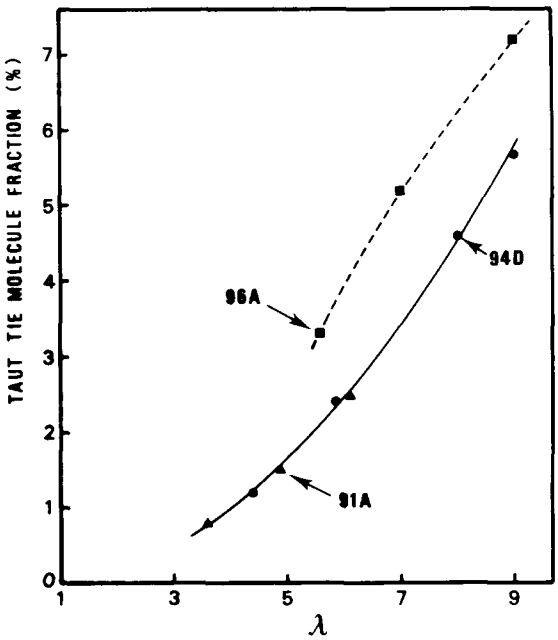

Fig. 19. Fraction of taut tie molecules as a function of draw ratio.

polyethylene of low or medium density, the taut tie molecules are assumed to be amorphous but have an axial Young's modulus equal to that of the crystals, i.e., $E_{\|}$ (tie molecule) = $E_{\|}$ (crystal) = 315 GPa.[34] We will analyze only the ultrasonic axial Young's modulus at −60°C, at which temperature the crystallinity dependence of the modulus for isotropic polyethylene is so weak that a reliable value for the amorphous phase E^a can be obtained by fitting the data between $X = 0.44$ and 0.8 to a series model. E^a is then found to be 2.8 GPa.

With these known parameters, the fraction of taut tie molecules b is calculated and shown as a function of draw ratio in Figure 19. Whereas the b values for Sclair 91A and 94D fall on the same curve the tie molecule fraction for Sclair 96A is about 30% higher. This is in contrast to the behavior of the amorphous orientation function f_a, which lies on the same curve for all three polymers (see Fig. 1). It is also noted that b and f_a have different draw ratio dependence, with b increasing much more substantially with draw ratio than f_a.

We are grateful to DuPont Canada Inc. for providing the polyethylene samples and Dr. H. C. Ng of DuPont Canada Inc. for enlightening discussion.

References

1. N. Fountas, *Plastics World*, (Feb.), 45 (1981).
2. C. L. Choy, W. P. Leung, and H. C. Ng, *J. Appl. Polym. Sci.*, **32**, 5883 (1986).
3. H. C. Ng, DuPont Canada Inc., private communication.
4. R. Seguela and F. Rietsch, *Polymer*, **27**, 703 (1986).
5. W. A. Lee and R. A. Rutherford, in *Polymer Handbook*, edited by J. Brandrup and E. H. Immergut, Wiley-Interscience, New York, 1975.

6. R. J. Samuels, *Structured Polymer Properties*, Wiley, New York, 1974.
7. B. Wunderlich and C. Cormier, *J. Polym. Sci., Polym. Phys. Ed.*, **5**, 987 (1967).
8. Z. W. Wilchinsky, in *Advances in X-Ray Analysis*, Plenum, New York, 1963, Vol. 6.
9. W. P. Leung and C. L. Choy, *J. Polym. Sci., Polym. Phys. Ed.*, **21**, 725 (1983).
10. G. R. Taylor and S. R. Darin, *J. Appl. Phys.*, **26**, 1075 (1955).
11. C. W. Bunn and R. de P. Daubeny, *Trans. Faraday Soc.*, **50**, 1173 (1954).
12. Y. Fukui, T. Asada, and S. Onogi, *Polym. J.*, **3**, 100 (1972).
13. K. Nakayama and H. Kanetsuna, *J. Mater. Sci.*, **10**, 1105 (1975).
14. M. Pietralla, H. P. Grossmann, and J. K. Kruger, *J. Polym. Sci., Polym. Phys. Ed.*, **20**, 1195 (1982).
15. N. G. McCrum, in *Molecular Basis of Transitions and Relaxations*, edited by D. J. Meier, Gordon and Breach, New York, 1978.
16. R. H. Boyd, *Polymer*, **26**, 323 (1985).
17. R. Popli, M. Glotin, and L. Mandelkern, *J. Polym. Sci., Polym. Phys. Ed.*, **22**, 407 (1984).
18. G. Raumann and D. W. Saunders, *Proc. Phys. Soc.*, **77**, 1028 (1961).
19. G. Raumann, *Proc. Phys. Soc.*, **79**, 1221 (1962).
20. V. B. Gupta and I. M. Ward, *J. Macromol. Sci., Phys.*, **B2**, 89 (1968).
21. Z. H. Stachurski and I. M. Ward, *J. Macromol. Sci., Phys.*, **B3**, 445 (1969).
22. A. J. Owens and I. M. Ward, *J. Macromol. Sci., Phys.*, **B19(1)**, 35 (1981).
23. C. L. Choy, W. P. Leung, and C. W. Huang, *Polym. Eng. Sci.*, **33**, 910 (1983).
24. C. L. Choy and W. P. Leung, *J. Polym. Sci., Polym. Phys. Ed.*, **23**, 1759 (1985).
25. N. H. Ladizesky and I. M. Ward, *J. Macromol. Sci., Phys.*, **B5**, 745 (1971).
26. J. C. Halpin and J. L. Kardos, *J. Appl. Phys.*, **43**, 2235 (1972).
27. J. L. Kardos and J. Raisoni, *Polym. Eng. Sci.*, **15**, 183 (1975).
28. T. T. Wang, *J. Appl. Phys.*, **44**, 2218 (1973).
29. R. L. McCullough, C. T. Wu, J. C. Seferis, and P. H. Lindenmeyer, *Polym. Eng. Sci.*, **16**, 371 (1976).
30. J. C. Seferis, R. L. McCullough, and R. J. Samuels, *Polym. Eng. Sci.*, **16**, 334 (1976).
31. S. W. Tsai, J. C. Halpin, and N. J. Pagano, Composite Materials Workshop, Technomic, Stamford, CT, 1968.
32. M. Takayanagi, K. Imada, and T. Kajiyama, *J. Polym. Sci.*, **C15**, 263 (1966).
33. I. M. Ward, in *Developments of Oriented Polymers-1*, edited by I. M. Ward, Applied Science, London, 1982.
34. K. Tashiro, M. Kobayashi, and H. Tadokoro, *Macromolecules*, **11**, 985 (1970).

Received August 17, 1987
Accepted August 24, 1987